JOURNAL OF THERMOPHYSICS AND HEAT TRANSFER
Vol. 24, No. 1, January–March 2010

Inverse Heat Conduction Using Measured Back Surface Temperature and Heat Flux

Jianhua Zhou,* Yuwen Zhang,† J. K. Chen,‡ and Z. C. Feng§
University of Missouri, Columbia, Missouri 65211

DOI: 10.2514/1.40549

In the high-energy laser heating of a target, the temperature and heat flux at the heated surface are not directly measurable, but they can be estimated by solving an inverse heat conduction problem based on the measured temperature and/or the heat flux at the accessible (back) surface. In this study, the one-dimensional inverse heat conduction problem in a finite slab is solved by the conjugate gradient method, using measured temperature and heat flux at the accessible (back) surface. Simulated measurement data are generated by solving a direct problem, in which the front surface of the slab is subjected to high-intensity periodic heating. Two cases are simulated and compared, with the temperature or heat flux at the heated front surface chosen as the unknown function to be recovered. The results show that the latter choice (i.e., choosing back surface heat flux as the unknown function) can give better estimation accuracy in the inverse heat conduction problem solution. The front surface temperature can be computed with high precision as a by-product of the inverse heat conduction problem algorithm. The robustness of this inverse heat conduction problem formulation is tested by different measurement errors and frequencies of the input periodic heating flux.

Nomenclature

a	=	thermal diffusivity, $a = k/(\rho c_p)$, m^2/s
c_p	=	specific heat, J/(kg K)
$d^k(t)$	=	direction of descent (nondimensional) at iteration level k
f	=	frequency of sinusoidal component of laser heating flux at front surface, Hz
h	=	convection heat transfer coefficient (nondimensional), defined in Eq. (1)
h^*	=	convection heat transfer coefficient, $W/(m^2\,K)$
k	=	thermal conductivity, W/(m K)
L	=	thickness of one-dimensional slab (nondimensional), defined in Eq. (1)
L^*	=	thickness of one-dimensional slab, m
l_c	=	characteristic length, m
$q[L, t; q_1(t)]$	=	computed heat flux at back surface (nondimensional) when front surface heat flux is $q_1(t)$
$q[L, t; T_1(t)]$	=	computed heat flux at back surface (nondimensional) when front surface temperature is $T_1(t)$
q_c^*	=	constant component in laser heating flux at front surface, W/m^2
$q_1(t)$	=	observed heat flux at front surface (nondimensional), $q_1(t) = q_1^*(t)l_c/(kT_c)$
$q_1^*(t)$	=	observed heat flux at front surface, W/m^2
q''	=	intensity of heating source at front surface (nondimensional), defined in Eq. (1)
q''^*	=	intensity of heating source at front surface, W/m^2
$q^*(L, t)$	=	calculated heat flux at back surface, based on the direct problem equations (36–39), W/m^2
S	=	objective function (nondimensional)
T	=	temperature (nondimensional), defined in Eq. (1)
T_c	=	characteristic temperature, K
$T[L, t; q_1(t)]$	=	computed temperature at back surface (nondimensional) when front surface heat flux is $q_1(t)$
$T[L, t; T_1(t)]$	=	computed temperature at back surface (nondimensional) when front surface temperature is $T_1(t)$
T_0	=	initial temperature (nondimensional), defined in Eq. (1)
T_0^*	=	initial temperature, K
$T_1(t)$	=	front surface temperature (nondimensional), $T_1(t) = T_1^*(t)/T_c$
$T_1^*(t)$	=	front surface temperature, K
T_∞	=	ambient temperature (nondimensional), defined in Eq. (1)
T_∞^*	=	ambient temperature, K
$T^*(L, t)$	=	calculated temperature at back surface, based on the direct problem equations (36–39), K
$T^*(x, t)$	=	temperature, K
t	=	time (nondimensional), defined in Eq. (1)
t_f	=	final time (nondimensional)
t_f^*	=	final time, s
t^*	=	time, s
x	=	spatial coordinate variable (nondimensional), defined in Eq. (1)
x^*	=	spatial coordinate variable, m
$Y(t)$	=	nondimensional measured data (temperature or heat flux), with errors at back surface obtained by numerical simulations: $Y(t) = Y^*(t)l_c/(kT_c)$ for heat flux and $Y(t) = Y^*(t)/T_c$ for temperature
$Y_{TL}(t)$	=	measured temperature at the back surface (nondimensional), $Y_{TL}(t) = Y_{TL}^*(t)/T_c$
$Y_{TL}^*(t)$	=	measured temperature at the back surface, K
$Y_{\text{exact}}(t)$	=	nondimensional measured data (temperature or heat flux) without errors at back surface obtained by numerical simulation, $Y_{\text{exact}}(t) = Y_{\text{exact}}^*(t)l_c/(kT_c)$ for heat flux, $Y_{\text{exact}}(t) = Y_{\text{exact}}^*(t)/T_c$ for temperature

Received 24 August 2008; revision received 14 September 2009; accepted for publication 26 September 2009.

*Research Assistant Professor, Department of Mechanical and Aerospace Engineering. Senior Member AIAA.
†Professor, Department of Mechanical and Aerospace Engineering. Associate Fellow AIAA (Corresponding Author).
‡William and Nancy Thompson Professor, Department of Mechanical and Aerospace Engineering.
§Professor, Department of Mechanical and Aerospace Engineering.

$Y_{qL}(t)$ = measured heat flux at the back surface (nondimensional), $Y_{qL}(t) = Y^*_{qL}(t)l_c/(kT_c)$
$Y^*_{qL}(t)$ = measured heat flux at the back surface, W/m^2
β^k = search step size (nondimensional) at iteration level k
γ^k = conjugate coefficient (nondimensional) at iteration level k
$\Delta q[L, t; d^k]$ = variation of heat flux (nondimensional) obtained by the sensitivity problem when the front surface temperature or heat flux is subjected to a perturbation d^k, $\Delta q = -\partial(\Delta T)/\partial x$
$\Delta S[T_1(t)]$ = small variation of objective function (nondimensional)
$\Delta T[x, t; d^k]$ = variation of temperature (nondimensional) obtained by the sensitivity problem when front surface temperature or heat flux is subjected to a perturbation d^k
ΔT_1 = variation of temperature at front surface (nondimensional)
δ = Dirac delta function
ε = surface emissivity
$\lambda(x, t)$ = Lagrange multiplier (nondimensional)
ρ = density, kg/m^3
σ = Stefan–Boltzmann constant (nondimensional), defined in Eq. (1)
σ^* = Stefan–Boltzmann constant, $\sigma = 5.67 \times 10^{-8}$ $W/(m^2 K^4)$
τ = transformation of the time variable (nondimensional)
ϕ = standard deviation of the measurements (nondimensional)
χ = tolerance used to stop the conjugate gradient method iteration procedure (nondimensional)
ω = random variable between 0 and 1
$\nabla S[T_1^k(t)]$ = gradient of objective function (nondimensional) at iteration level k

Superscripts

k = iteration level
$*$ = dimensional quantities

Subscripts

f = final
max = maximum value
q = heat flux
T = temperature
0 = initial

I. Introduction

HIGH-ENERGY laser weapons offer the advantage of remote delivery at the speed of light onto a small spot on a military target. During laser irradiation, it is critical to know the temperature at the heated front target surface in order to accurately understand the damage mechanism. However, the heated front surface is either inaccessible or so hot that it is unsuitable for attaching a sensor. A similar problem can also be encountered in some laser manufacturing processes [1]. Under these circumstances, the front surface temperature can be determined indirectly by solving an inverse heat conduction problem (IHCP) [2–4] based on the transient temperature or/and heat flux measured at the back surface.

In the mathematical formulation of the inverse problem, either temperature or heat flux can be measured at the back surface. Most previous researchers prefer temperature measurements, because temperature can be measured with fewer uncertainties as compared with heat flux measurements [5–8]. However, recent studies have shown that using measured heat flux as additional information in the formulation of an IHCP can increase the stability of the solution and is less prone to the inherent instability of the ill-posed problem of inverse heat conduction [9,10].

Although IHCPs have been extensively studied for different applications in the past (e.g., [11–19]), little work has been done for the inverse problem related to laser irradiation of a remote surface. The laser energy is delivered to the target surface in a periodic way because of laser or atmospheric variations. The periodic heat flux may pose extra difficulties in the solution of inverse problems. Because the formulation of the IHCP is quite subjective, it is necessary to determine which formulation is most appropriate for these applications.

In this study, a one-dimensional (1-D) IHCP in a finite slab is formulated and solved using the conjugate gradient method (CGM), with an adjoint problem being used for function estimation [3,4]. The inverse solution for the case in which the front surface of the slab is subjected to high-intensity periodic heating is illustrated to identify the most robust IHCP formulation for laser manufacturing applications. Both the temperature and heat flux are measured at the back surface. The former is used as the back surface boundary condition, whereas the latter is adopted in the objective function to be minimized. Two cases are examined in detail, in which the temperature or heat flux at the heated front surface is chosen as the unknown function to be recovered. The most robust and error-insensitive IHCP formulation will be proposed.

II. Model Description

For the case that the laser beam size is much larger than the thickness of the wall, one can treat the inverse heat transfer problem as 1-D. To illustrate the methodology of the inverse heat transfer algorithms used in this study, a finite slab with a thickness of L^* (as shown in Fig. 1) is considered. Initially, the slab has a uniform temperature of T_0^*. From $t^* > 0$, the front surface of the slab is subjected to high-intensity laser heating. The purpose of the inverse problem is to reconstruct the heating condition at the front surface, based on the measured temperature and heat flux at the back surface. Because of the fact that the temperature measurement data contain fewer errors as compared with the heat flux measurements [5–8], the temperature $Y^*_{TL}(t)$ is used as the boundary condition, and the heat flux $Y^*_{qL}(t)$ is incorporated into the objective function. It is assumed that the density, specific heat, and thermal conductivity of the slab are constants.

Two cases (i.e., case 1 and case 2, as shown in Figs. 1a and 1b, respectively) are examined in order to test which quantity (temperature or heat flux) is more appropriate to be employed as the unknown to be recovered, such that the best accuracy can be achieved.

In the following, the mathematical formulations for different cases will be described. To this end, the following dimensionless quantities are defined:

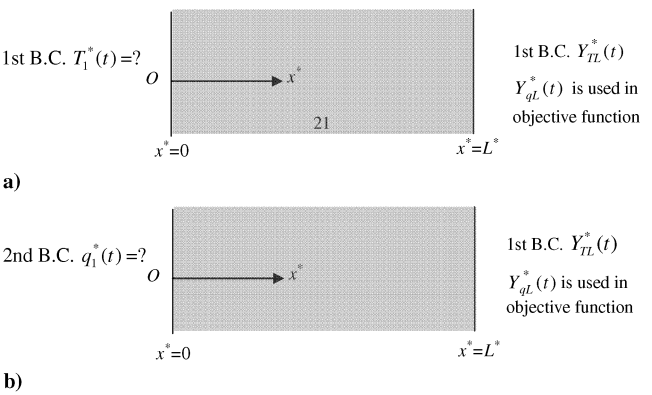

Fig. 1 Physical models of a) case 1: recovering the front surface temperature $T_1^*(t)$ and b) case 2: recovering the front surface heat flux $q_1^*(t)$ (B.C. denotes boundary condition).

$$T = \frac{T^*}{T_c}, \qquad T_\infty = \frac{T^*_\infty}{T_c}, \qquad T_0 = \frac{T^*_0}{T_c}$$
$$x = \frac{x^*}{l_c}, \qquad L = \frac{L^*}{l_c}, \qquad t = \frac{at^*}{l_c^2}$$
$$q'' = \frac{q''^* l_c}{kT_c}, \qquad h = \frac{h^* l_c}{k}, \qquad \sigma = \frac{\sigma^* T_c^3 l_c}{k} \tag{1}$$

where the quantities with the superscript $*$ denote the dimensional quantities, whereas the quantities without the superscript $*$ represent the nondimensional quantities. In the remainder of this paper, all the equations are expressed in nondimensional form unless otherwise specified.

A. Direct Problem

1. Case 1

For this case, the front surface temperature is chosen as the unknown to be recovered (Fig. 1a). The direct problem for this case can be expressed as follows:

$$\frac{\partial T}{\partial t} = \frac{\partial^2 T}{\partial x^2} \tag{2}$$

in $0 < x < L$ for $t > 0$,

$$T(x,\ 0) = T_0 \tag{3}$$

in $0 < x < L$ for $t = 0$,

$$T(0,\ t) = T_1(t) \tag{4}$$

at $x = 0$ for $t > 0$, and

$$T(L,\ t) = Y_{TL}(t) \tag{5}$$

at $x = L$ for $t > 0$, where $T_1(t)$ is the nondimensional front surface temperature and $Y_{TL}(t)$ is the nondimensional measured temperature at the back surface.

In the direct problem associated with the physical problem described previously, the front surface temperature $T_1(t)$ and the back surface temperature $Y_{TL}(t)$ are considered to be known. The objective of the direct problem is then to determine the transient temperature distribution in the slab.

2. Case 2

For this case, the front surface heat flux is chosen as the unknown to be recovered (Fig. 1b). The mathematical formulation is almost the same as those in Eqs. (2–5), except that the boundary condition at $x = 0$ is replaced by

$$-\frac{\partial T(0,\ t)}{\partial x} = q_1(t) \tag{6}$$

at $x = 0$ for $t > 0$, where $q_1(t)$ is the nondimensional front surface heat flux.

B. Inverse Problem

For the inverse problem, the boundary condition at $x = 0$ is unknown, but everything else in the corresponding direct problem is known. The additional information needed in recovering the front surface boundary condition is available from the readings of a heat flux sensor installed at the back surface.

1. Case 1

The inverse problem for this case can be expressed as follows:

$$\frac{\partial T}{\partial t} = \frac{\partial^2 T}{\partial x^2} \tag{7}$$

in $0 < x < L$ for $t > 0$,

$$T(x,\ 0) = T_0 \tag{8}$$

in $0 < x < L$ for $t = 0$, and

$$T(L,\ t) = Y_{TL}(t) \tag{9}$$

at $x = L$ for $t > 0$, where the front surface temperature $T_1(t)$ is regarded as unknown. The heat flux readings at the back surface $Y_{qL}(t)$ are considered available as additional information.

The solution of the inverse problem will be obtained in such a way that the following objective function is minimized (for continuously measured data):

$$S[T_1(t)] = \int_0^{t_f} \{Y_{qL}(t) - q[L,\ t;\ T_1(t)]\}^2\, \mathrm{d}t \tag{10}$$

where $Y_{qL}(t)$ and $q[L,\ t;\ T_1(t)]$ are the nondimensional measured and computed heat fluxes at the back surface, respectively.

2. Case 2

The governing equations of the inverse problem for this case are the same as those in case 1 [i.e., Eqs. (7–9)]. The only difference is that the heat flux at the front surface $q_1(t)$ is regarded as unknown, and the following objective function is minimized:

$$S[q_1(t)] = \int_0^{t_f} \{Y_{qL}(t) - q[L,\ t;\ q_1(t)]\}^2\, \mathrm{d}t \tag{11}$$

where $Y_{qL}(t)$ is known as the measured heat flux at the back surface.

C. Conjugate Gradient Method for Minimization

The iterative process based on the CGM [3,4] is now derived for the estimation of the unknown temperature $[T_1(t)]$ or heat flux $[q_1(t)]$ by minimizing the objective function S.

The iterative process for case 1 is as follows:

$$T_1^{k+1}(t) = T_1^k(t) - \beta^k d^k(t) \tag{12}$$

where β^k is the search step size in going from iteration k to iteration $k + 1$, and $d^k(t)$ is the direction of descent (i.e., search direction) given by

$$d^k(t) = \nabla S[T_1^k(t)] + \gamma^k d^{k-1}(t) \tag{13}$$

which is a conjugate of the gradient direction $\nabla S[T_1^k(t)]$ at iteration k and the direction of descent $d^{k-1}(t)$ at iteration $k - 1$. The conjugate coefficient γ^k is determined from

$$\gamma^k = \left(\int_0^{t_f} \nabla S[T_1^k(t)]\{\nabla S[T_1^k(t)] - \nabla S[T_1^{k-1}(t)]\}\, \mathrm{d}t \right) \Big/ \left(\int_0^{t_f} \{\nabla S[T_1^{k-1}(t)]\}^2\, \mathrm{d}t \right) \tag{14}$$

with $\gamma^0 = 0$

The iterative process for case 2 can be obtained by replacing $T_1^{k-1}(t)$, $T_1^k(t)$, and $T_1^{k+1}(t)$ with $q_1^{k-1}(t)$, $q_1^k(t)$, and $q_1^{k+1}(t)$, respectively, in Eqs. (12–14).

To perform the iterations according to Eq. (12), we need to compute the step size β^k and the gradient of the functional $\nabla S[T_1^k(t)]$. To develop expressions for the determination of these two quantities,

a sensitivity problem and an adjoint problem for each case are constructed below.

D. Sensitivity Problem and Search Step Size

1. Case 1

The sensitivity problem is obtained from the original direct problem [Eqs. (2–5) for Case 1] in the following manner. It is assumed that when $T_1(t)$ undergoes a variation ΔT_1, T is perturbed by ΔT. Then, by replacing T_1 with $T_1 + \Delta T_1$ and T with $T + \Delta T$ in the direct problem, subtracting the direct problem from the resulting expressions, and neglecting the second-order terms, the sensitivity problem for the sensitivity function ΔT can be obtained.

The sensitivity problem for case 1 can be expressed as

$$\frac{\partial \Delta T}{\partial t} = \frac{\partial^2 \Delta T}{\partial x^2} \tag{15}$$

in $0 < x < L$ for $t > 0$,

$$\Delta T(x,\ 0) = 0 \tag{16}$$

in $0 < x < L$ for $t = 0$,

$$\Delta T(0,\ t) = \Delta T_1(t) \tag{17}$$

at $x = 0$ for $t > 0$, and

$$\Delta T(L,\ t) = 0 \tag{18}$$

at $x = L$ for $t > 0$.

The objective function for iteration $k + 1$ is obtained by rewriting Eq. (10) as

$$S[T_1^{k+1}(t)] = \int_0^{t_f} \{Y_{qL}(t) - q[L,\ t;\ (T_1^k - \beta^k d^k)]\}^2\, \mathrm{d}t \tag{19}$$

where T_1^{k+1} is replaced by the expression given by Eq. (12). If $q[L,\ t;\ (T_1^k - \beta^k d^k)]$ is linearized by a Taylor expansion, Eq. (19) takes the following form:

$$S[T_1^{k+1}(t)] = \int_0^{t_f} \{Y_{qL}(t) - q[L,\ t;\ T_1^k] - \beta^k \Delta q(L,\ t;\ d^k)\}^2\, \mathrm{d}t \tag{20}$$

where $q[L,\ t;\ T_1^k]$ is the solution of the direct problem [Eqs. (2–5)] by using the estimated T_1^k at $x = 0$ and time t. The sensitivity function $\Delta q(L,\ t;\ d^k)$ is taken as the result of the solution of Eqs. (15–18) at the measured position $x = L$ and at time t by letting $\Delta T_1 = d^k$. The search step size β^k is determined by minimizing the function given by Eq. (20) with respect to β^k. The following expression results:

$$\beta^k = \left(\int_0^{t_f} \{q[L,\ t;\ T_1^k] - Y_{qL}(t)\} \Delta q[L,\ t;\ d^k(t)]\, \mathrm{d}t \right) \Big/ \left(\int_0^{t_f} \{\Delta q[L,\ t;\ d^k(t)]\}^2\, \mathrm{d}t \right) \tag{21}$$

2. Case 2

For this case, the mathematical expression of the sensitivity problem is almost the same as that in Eqs. (15–18), except that the boundary condition at $x = 0$ is changed to

$$-\frac{\partial \Delta T(0, t)}{\partial x} = \Delta q_1(t) \tag{22}$$

at $x = 0$ for $t > 0$.

The search step size β^k for this case can be obtained by replacing $T_1(t)$ with $q_1(t)$ in Eqs. (19–21).

E. Adjoint Problem and Gradient Equation

1. Case 1

To obtain the adjoint problem, Eqs. (2–5) are multiplied by the Lagrange multiplier $\lambda(x,\ t)\, \mathrm{d}x\, \mathrm{d}t$, and the resulting expression is integrated over the corresponding space and time domains. Then, the result is added to the right-hand side of Eq. (10) to yield the following expression for the objective function:

$$S[T_1(t)] = \int_0^{t_f} \{Y_{qL}(t) - q[L,\ t;\ T_1(t)]\}^2\, \mathrm{d}t + \int_0^{t_f} \int_0^L \lambda(x,\ t) \left[\frac{\partial^2 T}{\partial x^2} - \frac{\partial T}{\partial t} \right] \mathrm{d}x\, \mathrm{d}t \tag{23}$$

The variation ΔS is obtained by perturbing T_1 by ΔT_1, T by ΔT, and q by Δq in Eq. (23). Subtracting from the resulting expression the original Eq. (23) and neglecting the second-order terms, one finds

$$\Delta S[T_1(t)] = \int_0^{t_f} \int_0^L 2\{q[x,\ t;\ T_1(t)] - Y_{qL}(t)\} \Delta q(x,\ t) \delta(x - L)\, \mathrm{d}x\, \mathrm{d}t + \int_0^{t_f} \int_0^L \lambda(x,\ t) \left[\frac{\partial^2 \Delta T}{\partial x^2} - \frac{\partial \Delta T}{\partial t} \right] \mathrm{d}x\, \mathrm{d}t \tag{24}$$

where $\delta(\,)$ is the Dirac delta function. In Eq. (24), the domain integral term is reformulated based on integration by parts as follows:

$$\begin{aligned} &\int_0^L \lambda(x,\ t) \frac{\partial^2 \Delta T}{\partial x^2}\, \mathrm{d}x \\ &= \left[\lambda(x,\ t) \frac{\partial [\Delta T(x, t)]}{\partial x} - \frac{\partial [\lambda(x, t)]}{\partial x} \Delta T(x,\ t) \right]_{x=0}^{x=L} \\ &+ \int_{x=0}^{x=L} \Delta T(x,\ t) \frac{\partial^2 [\lambda(x,\ t)]}{\partial x^2}\, \mathrm{d}x = \lambda(L,\ t) \frac{\partial [\Delta T(L,\ t)]}{\partial x} \\ &- \frac{\partial [\lambda(L,\ t)]}{\partial x} \Delta T(L,\ t) - \lambda(0,\ t) \frac{\partial [\Delta T(0,\ t)]}{\partial x} \\ &+ \frac{\partial [\lambda(0,\ t)]}{\partial x} \Delta T(0,\ t) + \int_{x=0}^{x=L} \Delta T(x,\ t) \frac{\partial^2 [\lambda(x,\ t)]}{\partial x^2}\, \mathrm{d}x \end{aligned} \tag{25}$$

$$\begin{aligned} &\int_0^{t_f} \lambda(x,\ t) \frac{\partial \Delta T}{\partial t}\, \mathrm{d}t = [\lambda(x,\ t) \Delta T(x,\ t)]_{t=0}^{t=t_f} \\ &- \int_{t=0}^{t=t_f} \Delta T(x,\ t) \frac{\partial [\lambda(x,\ t)]}{\partial t}\, \mathrm{d}t = \lambda(x,\ t_f) \Delta T(x,\ t_f) \\ &- \lambda(x,\ 0) \Delta T(x,\ 0) - \int_{t=0}^{t=t_f} \Delta T(x,\ t) \frac{\partial [\lambda(x,\ t)]}{\partial t}\, \mathrm{d}t \end{aligned} \tag{26}$$

In Eqs. (25) and (26), $\Delta T(x,\ 0)$, $\Delta T(0,\ t)$, and $\Delta T(L,\ t)$ can be replaced by 0, $\Delta T_1(t)$, and 0, respectively, according to the initial and boundary conditions of the sensitivity problem [i.e., Eqs. (16–18)]. After doing this, Eqs. (25) and (26) become

$$\begin{aligned} &\int_0^L \lambda(x,\ t) \frac{\partial^2 \Delta T}{\partial x^2}\, \mathrm{d}x = \lambda(L,\ t) \frac{\partial [\Delta T(L,\ t)]}{\partial x} \\ &- \lambda(0,\ t) \frac{\partial [\Delta T(0,\ t)]}{\partial x} + \frac{\partial [\lambda(0,\ t)]}{\partial x} \Delta T_1(t) \\ &+ \int_{x=0}^{x=L} \Delta T(x,\ t) \frac{\partial^2 [\lambda(x,\ t)]}{\partial x^2}\, \mathrm{d}x \end{aligned} \tag{27}$$

$$\begin{aligned} &\int_0^{t_f} \lambda(x,\ t) \frac{\partial \Delta T}{\partial t}\, \mathrm{d}t = \lambda(x,\ t_f) \Delta T(x,\ t_f) \\ &- \int_{t=0}^{t=t_f} \Delta T(x,\ t) \frac{\partial [\lambda(x,\ t)]}{\partial t}\, \mathrm{d}t \end{aligned} \tag{28}$$

Substitution of Eqs. (27) and (28) into Eq. (24) yields:

$$\Delta S[T_1(t)] = \int_0^{t_f}\int_0^L 2\{q[x,\,t;\,T_1(t)] - Y_{qL}(t)\}\Delta q(x,\,t)\delta(x-L)\,\mathrm{d}x\,\mathrm{d}t + \int_0^{t_f}\left\{\lambda(L,t)\frac{\partial[\Delta T(L,t)]}{\partial x} - \lambda(0,t)\frac{\partial[\Delta T(0,\,t)]}{\partial x} + \frac{\partial[\lambda(0,\,t)]}{\partial x}\Delta T_1(t) + \int_0^L \Delta T(x,\,t)\frac{\partial^2[\lambda(x,\,t)]}{\partial x^2}\,\mathrm{d}x\right\}\mathrm{d}t + \int_0^L\left\{\lambda(x,\,t_f)\Delta T(x,\,t_f) - \int_0^{t_f}\Delta T(x,\,t)\frac{\partial[\lambda(x,\,t)]}{\partial t}\,\mathrm{d}t\right\}\mathrm{d}x = \int_0^{t_f}\int_0^L 2\Delta T(x,\,t)\{q[x,\,t;\,T_1(t)] - Y_{qL}(t)\}\frac{\Delta q(x,\,t)}{\Delta T(x,\,t)}\delta(x-L)\,\mathrm{d}x\,\mathrm{d}t + \int_0^{t_f}\left\{\lambda(L,\,t)\frac{\partial[\Delta T(L,\,t)]}{\partial x} - \lambda(0,\,t)\frac{\partial[\Delta T(0,\,t)]}{\partial x} + \frac{\partial[\lambda(0,\,t)]}{\partial x}\Delta T_1(t)\right\}\mathrm{d}t + \int_0^{t_f}\int_0^L \Delta T(x,\,t)\frac{\partial^2[\lambda(x,\,t)]}{\partial x^2}\,\mathrm{d}x\,\mathrm{d}t - \int_0^L \lambda(x,\,t_f)\Delta T(x,\,t_f)\,\mathrm{d}x + \int_0^{t_f}\int_0^L \Delta T(x,\,t)\frac{\partial[\lambda(x,\,t)]}{\partial t}\,\mathrm{d}x\,\mathrm{d}t \tag{29}$$

The vanishing of the integrands containing $\Delta T(x,\,t)$ leads to the following differential equation:

$$\frac{\partial\lambda}{\partial t} + \frac{\partial^2\lambda}{\partial x^2} + 2\{q[x,\,t;\,T_1(t)] - Y_{qL}(t)\}\frac{\Delta q[x,\,t;\,d^k]}{\Delta T[x,\,t;\,d^k]}\delta(x-L) = 0 \tag{30}$$

where $\Delta T(x,\,t)$ and $\Delta q(x,\,t)$ are expressed as $\Delta T[x,\,t;\,d^k]$ and $\Delta q[x,\,t;\,d^k]$, respectively, because these two quantities are obtained by solving the sensitivity problem by letting $\Delta T_1(t) = d^k(t)$ in Eq. (17).

The vanishing of $\lambda(L,\,t)$, $\lambda(0,\,t)$, and $\lambda(x,\,t_f)$ in Eq. (29) results in

$$\lambda(x,\,t_f) = 0 \tag{31}$$

in $0 < x < L$ for $t = t_f$,

$$\lambda(0,\,t) = 0 \tag{32}$$

at$x = 0$ for $t > 0$, and

$$\lambda(L,\,t) = 0 \tag{33}$$

at $x = L$ for $t > 0$. Equations (30–33) constitute the boundary value problem for the Lagrange multiplier $\lambda(x,\,t)$, which is referred to as the adjoint problem.

The adjoint problem defined by Eqs. (30–33) is different from the standard initial value problem, in that the final time condition at time $t = t_f$ is specified instead of the customary initial condition. However, this problem can be transformed to an initial value problem by the transformation of the time variables as $\tau = t_f - t$.

After the definition of the adjoint problem [i.e., Eqs. (30–33)], only one term is left in Eq. (29); that is,

$$\Delta S[T_1(t)] = \int_0^{t_f}\frac{\partial[\lambda(0,\,t)]}{\partial x}\Delta T_1(t)\,\mathrm{d}t \tag{34}$$

By invoking the hypothesis that the unknown function $T_1(t)$ belongs to the space of square integrable functions in the domain $0 < t < t_f$, we can write [20]

$$\Delta S[T_1(t)] = \int_0^{t_f}\nabla S[T_1(t)]\Delta T_1(t)\,\mathrm{d}t \tag{35}$$

A comparison of Eqs. (29) and (30) leads to the following expression for the gradient of functional $S[T_1(t)]$:

$$\nabla S[T_1(t)] = \frac{\partial[\lambda(0,\,t)]}{\partial x} \tag{36}$$

2. Case 2

The adjoint problem for this case 1 is almost the same as that in Eqs. (30–33), except for the boundary condition at $x = 0$:

$$-\frac{\partial[\lambda(0,\,t)]}{\partial x} = 0 \tag{37}$$

at $x = 0$ for $t > 0$. The gradient of functional $S[q_1(t)]$ is the same as Eq. (36).

F. Stopping Criterion

Following the recommendations of [3,4], the discrepancy principle is used as the stopping criterion (for case 1). In the discrepancy principle, the iterative procedure is stopped when the following criterion is satisfied:

$$S[T_1(t)] < \chi \tag{38}$$

where χ denotes the tolerance.

It is assumed that the absolute value of the heat flux residuals may be approximated by

$$|Y_{qL}(t) - q[L,t;T_1(t)]| \approx \phi \tag{39}$$

where ϕ is the standard deviation of the measurements. Substituting Eq. (39) into Eq. (10), the following tolerance χ is obtained:

$$\chi = \phi^2 t_f \tag{40}$$

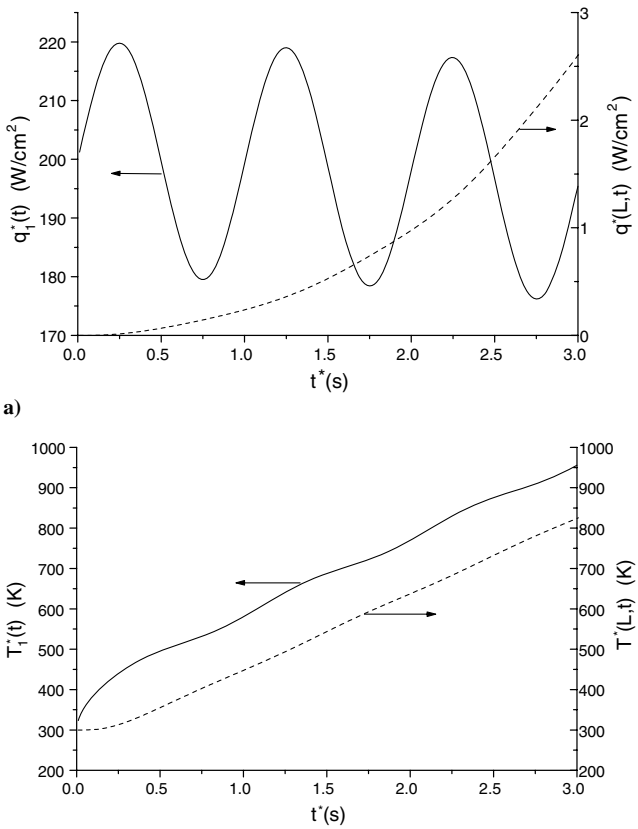

Fig. 2 Calculated results for the direct problem described by Eqs. (36–39): a) heat fluxes at front and back surfaces; and b) temperatures at front and back surfaces.

The stopping criterion is then given by Eq. (38) with χ determined from Eq. (40). The stopping criterion for case 2 can be obtained in a similar way.

III. Computational Procedure

Taking case 1 as an example, the computational procedure for the solution of this inverse problem using CGM may be summarized as follows.

Suppose an initial guess $T_1^0(t)$ is available for the function $T_1(t)$. Set $k = 0$ and then see the following steps:

1) Solve the direct problem given by Eqs. (2–5) and compute $T(x, t)$ based on $T_1^k(t)$.

2) Check the stopping criterion, Eq. (38). Continue if not satisfied.

3) Solve the adjoint problem given by Eqs. (30–33) for $\lambda(x, t)$.

4) Compute the gradient of the functional $\nabla S[T_1(t)]$ from Eq. (36).

5) Compute the conjugate coefficient γ^k and direction of descent $d^k(t)$ from Eqs. (13) and (14), respectively.

6) Set $\Delta T_1^k(t) = d^k(t)$ and solve the sensitivity problem given by Eqs. (15–18) for $\Delta T(x, t)$.

7) Compute the search step size β^k from Eq. (21).

8) Compute the new estimate for $T_1^{k+1}(t)$ from Eq. (12) and return to the first step.

One of the advantages of using the CGM to solve inverse problems is that the initial guess (i.e., $T_1^0(t)$) of the unknown quantities can be chosen arbitrarily. In all of the simulation cases considered in this study, the initial guess is taken as zero for convenience.

IV. Results and Discussion

A. Generation of Measurement Data

In the inverse problems considered in this study, estimation of the front surface heating condition is based on the measured data at the back surface. The measured temperature and heat flux at the back surface are generated based on the numerical simulation of the following direct problem:

$$\frac{\partial T}{\partial t} = \frac{\partial^2 T}{\partial x^2} \tag{41}$$

in $0 < x < L$ for $t > 0$,

$$T(x, 0) = T_0 \tag{42}$$

in $0 < x < L$ for $t = 0$,

$$-\frac{\partial T(L, t)}{\partial x} = q'' - h(T - T_\infty) - \varepsilon\sigma(T^4 - T_\infty^4) \tag{43}$$

at $x = 0$ for $t > 0$, and

$$-\frac{\partial T(L, t)}{\partial x} = h(T - T_\infty) + \varepsilon\sigma(T^4 - T_\infty^4) \tag{44}$$

at $x = L$ for $t > 0$, where q'' is the nondimensional periodic heat flux imposed at the front surface, h is the nondimensional convection heat transfer coefficient at the front and back surfaces, T_∞ is the nondimensional ambient temperature, ε is the surface emissivity, and σ is the nondimensional Stefan–Boltzmann constant. This direct problem is numerically solved by the computer code that has been verified in our previous work [20].

By solving Eqs. (41–44), the heat fluxes and temperatures at both the front and back surfaces can be obtained. The front surface temperature and heat fluxes will be used as exact solutions to examine the accuracy of the inverse heat conduction algorithm. The back surface temperature and heat flux will be used as boundary conditions and employed in the objective functions, Eqs. (10) and (11), respectively.

Real measurements generally contain errors. We assume normally distributed uncorrelated errors having a mean value of zero and a constant standard deviation. Therefore, measurements containing random errors are simulated by adding a random noise (error term) of the form

$$Y(t) = Y_{\text{exact}}(t) + \omega\phi \tag{45}$$

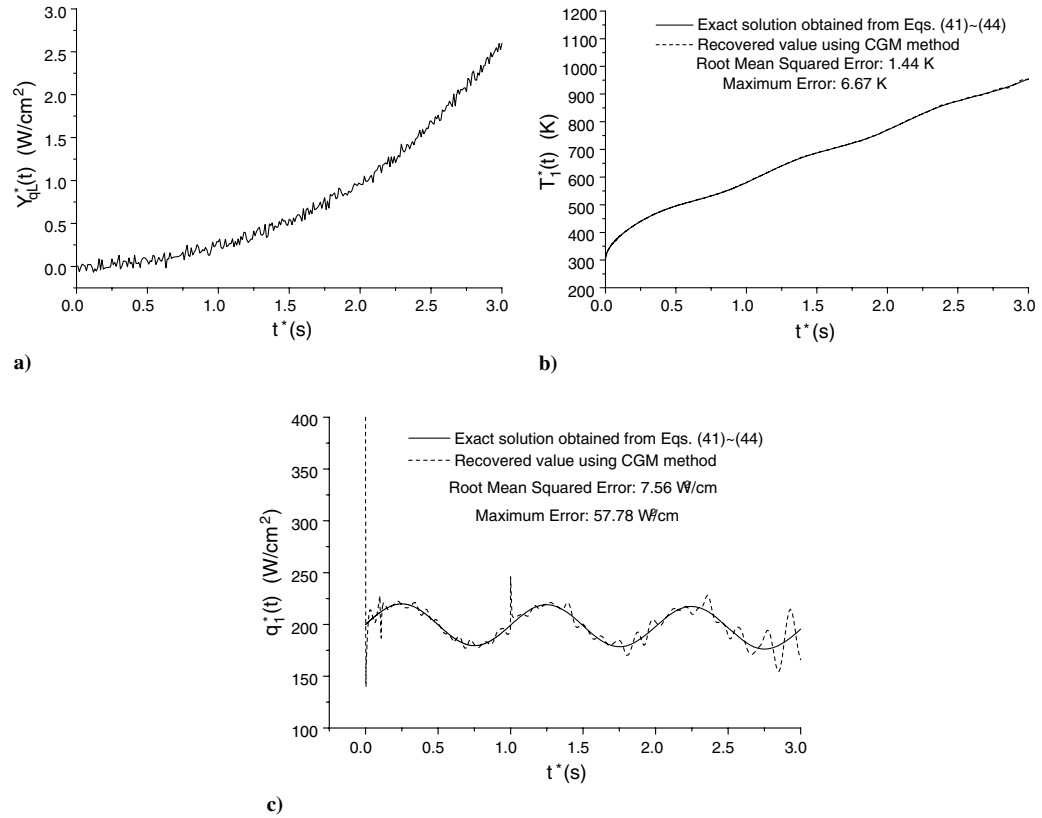

Fig. 3 Calculated results for case 1: a) back surface heat flux measurements (with 1% measurement errors); b) estimated front surface temperature by CGM inverse method; and c) front surface heat flux as a by-product.

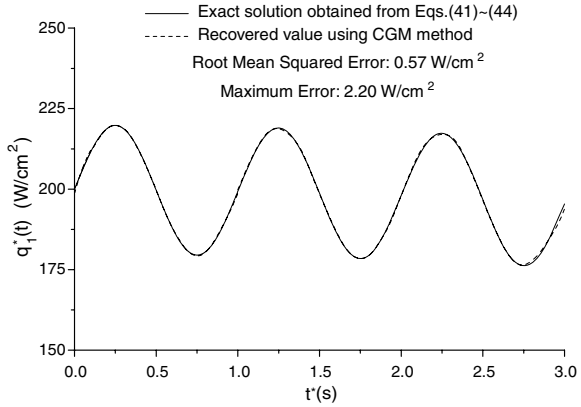

a)

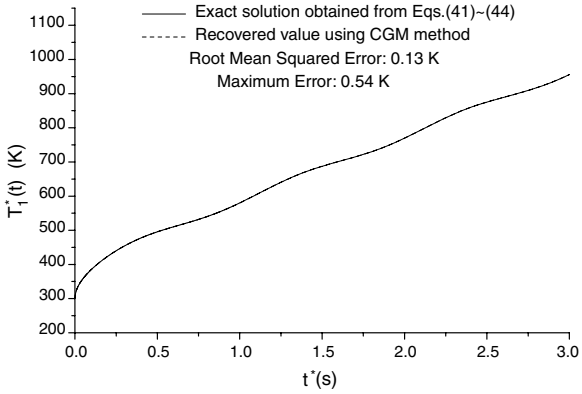

b)

Fig. 4 Calculated results for case 2: a) estimated front surface heat flux by CGM inverse method; and b) front surface temperature as a by-product.

where $Y(t)$ is the simulated experimental data that are obtained from the solution of the direct problem [Eqs. (41–44)], and ϕ is the standard deviation of the measurements. In this study, ϕ is set as a percentage (1–10%) of the highest measurement value at the back surface, and ω is a random variable between 0 and 1 generated by the Mersenne Twister method [21].

B. Results of Direct Problem

In the following simulations, the following thermal properties are used: $\rho = 7600$ kg/m^3, $c_p = 550$ J/(kg K), and $k = 18$ W/(m-K). Other parameters are $L^* = 2.5$ mm, $T_0^* = 300$ K, $T_\infty^* = 300$ K, $h^* = 5$ W/(m^2 K), and $\varepsilon = 0.92$. The front surface heat flux is assumed to be $q''^* = q_c^* + 0.1q_c^* \sin(2\pi f t^*)$ (W/m^2), where q_c^* is a constant heat flux that represents the heat flux intensity level at the front surface and f is the frequency of the sinusoidal component. This type of heat flux is intentionally used to represent a general periodic heating condition, although traditional lasers usually have a Gaussian or flat beam profile in time. Unless specified otherwise, the following simulation parameters are used: heat flux intensity level $q_c^* = 200$ W/cm^2, frequency of the sinusoidal component $f =$ 1.0 Hz, and standard deviation of the heat flux measurements $\delta = 1\%[Y_{qL}(t)]_{\max}$. It is assumed that there are no errors in the temperature measurements $[Y_{TL}(t)]$. The characteristic temperature T_c is set as 2000 K, and the characteristic length l_c is equal to the slab thickness (i.e., $l_c = L^*$).

Figure 2 shows the results for the direct problem described by Eqs. (36–39). It can be seen from Fig. 2b that there are some fluctuations in the front surface temperature because the front surface is subjected to a sinusoidal heat flux (Fig. 2a). However, no fluctuations are observed in the back surface heat flux (Fig. 2a) and temperature (Fig. 2b) due to damping and delay effects from heat diffusion. In Fig. 2, it appears that the final simulation time t_f^* is 3.0 s. But, the actual final time is taken as $t_f^* = 3.6$ s. The reason is as follows. For the CGM, the gradient is zero for some cases at the final time. For this situation, the initial guess used for $T_1(t)$ or $q_1(t)$ is never changed by the iterative procedure, generating instabilities in the solution in the neighborhood of t_f^*. One approach to overcome

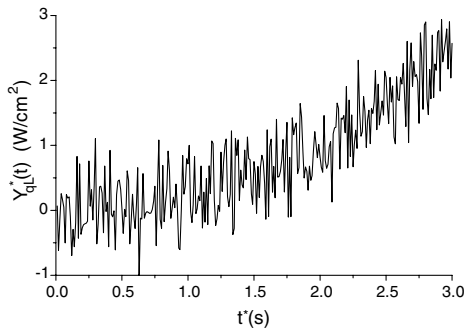

a)

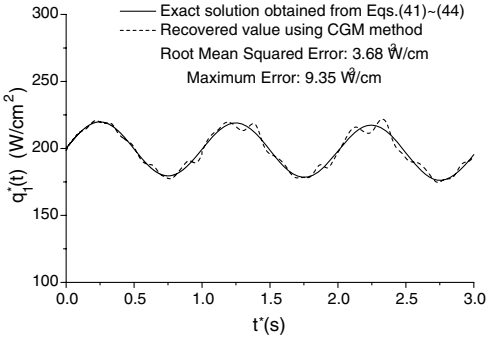

b)

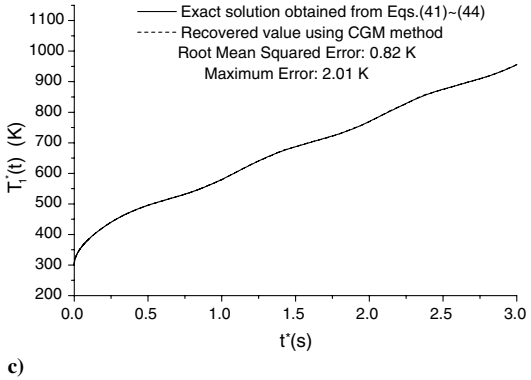

c)

Fig. 5 Effect of heat flux measurement error on the recovery accuracy for case 2: a) back surface heat flux measurements (with 10% measurement errors); b) estimated front surface heat flux by CGM inverse method; and c) front surface temperature as a by-product.

such difficulties is to consider a final time longer than that of interest [4]. Therefore, we used $t_f^* = 3.6$ s for the simulations in Fig. 2.

C. Comparison of Cases 1 and 2

Figure 3 shows the results for case 1. Figure 3a gives the measured heat flux at the back surface obtained by adding a 1% random error via Eq. (40). Figures 3b and 3c compare the inverse solutions and the exact solutions obtained from the solution of Eqs. (36–39). The rms error and maximum error between the inverse solution and exact solution are given. As is seen in Fig. 3b, the recovered temperature at the front surface agrees well with the exact solution obtained from the solution of Eqs. (36–39). But the estimation of the front surface heat flux as a by-product of the CGM algorithm is not satisfactory because there are very large errors around time $t^* = 0$ (maximum error is 57.78 W/cm^2, excluding those at $t^* = 0$, as indicated in Fig. 3c).

Figure 4 shows the calculated results for case 2. The measured heat flux at the back surface has the same error (1%) as in Fig. 3 and therefore is not shown here. It is seen from Fig. 4 that the maximum errors in heat flux and temperature are 2.20 W/cm^2 and 0.54 K, respectively. These values are much smaller than those presented in Fig. 3. This indicates that both the recovered temperature and the by-product heat flux at the front surface are in excellent agreement with the exact solutions. Therefore, compared with case 1, case 2 provides the most robust numerical scheme for the inverse estimation of the front surface heating condition based on measurement data at the back surface. It should be pointed out that no prior information about the front heating condition is required in the CGM algorithm used in this study.

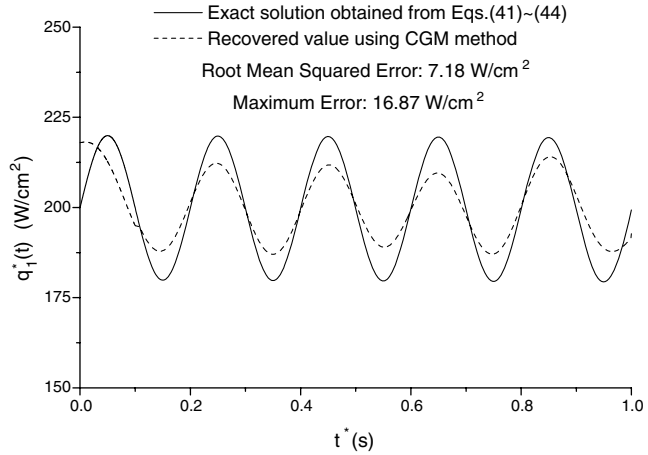

a)

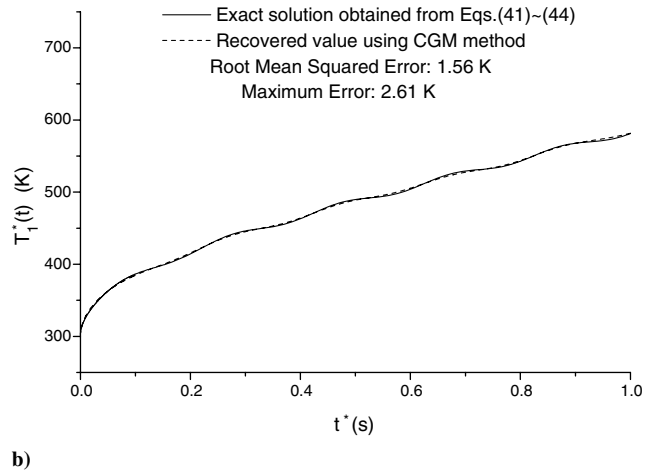

b)

Fig. 6 Effect of frequency of sinusoidal component on the recovery accuracy for case 2 ($f = 5$ Hz): a) estimated front surface heat flux by CGM inverse method; and b) front surface temperature as a by-product.

D. Parametric Study for Case 2

A powerful numerical scheme for inverse heat transfer should be stable even when the measured data contain considerable random errors. Figure 5 presents the effect of the heat flux measurement error on the accuracy of the IHCP formulation described by case 2. The simulation parameters are almost the same as those in Fig. 4, except that the random error of the measured heat flux is increased. It can be seen by comparing Figs. 4 and 5 that, when the heat flux measurement error is increased from 1% to 10%, the rms error in heat flux changes from 0.57 W/cm^2 to 3.68 W/cm^2 (Fig. 4a and 5b), and the rms error in the temperature rises from 0.13 to 0.82 K (Fig. 4b and 5c). Therefore, the IHCP formulation of case 2 proposed in this study has a good stability in the measurement uncertainty range (up to 10%) considered in this study.

Figure 6 presents the effect of the frequency of the sinusoidal component on the recovery accuracy of the IHCP formulation involved in case 2. The simulation parameters are almost the same as those in Fig. 4, except for the frequency of the sinusoidal component. It is found from Fig. 6a that, when the frequency f is increased to 5 Hz, the frequency of the estimated heat flux (about 4.88 Hz) agrees well with that of the exact frequency (5 Hz), and there is little decrease in the accuracy of the amplitude of the recovered heat flux signal. The maximum error in the heat flux amplitude is 16.87 W/cm^2, as shown in Fig. 6a. Considering the heat flux level used in this study is as high as 200 W/cm^2, we can think the inverse heat flux solution presented in Fig. 6a is still good. Again, the front surface temperature can be recovered with good accuracy as a by-product of the inverse algorithm (Fig. 6b).

V. Conclusions

A CGM algorithm is proposed to reconstruct the heat flux and temperature at the front surface of a finite slab that is subjected to high-intensity heating. To achieve high recovery accuracy, both the temperature and heat flux are measured at the back surface. The temperature measurement data are used as the back surface boundary condition, whereas the heat flux is employed in the objective function. Two cases are examined in detail: 1) the front surface temperature is chosen as the unknown to be recovered, and 2) the front surface heat flux is chosen as the unknown to be recovered. The sensitivity problems and adjoint problems for the two cases are derived and formulated. A CGM iterative numerical procedure is established, aiming to obtain a convergent IHCP solution. The results showed that better accuracy on the recovered front surface boundary condition can be obtained when the front surface heat flux is chosen as the unknown to be recovered (case 2). Consequently, the front surface heat flux (instead of the front surface temperature) should be recovered when both the back surface temperature and the heat flux are known. The robustness of the suggested IHCP formulation (case 2) is tested for some different cases, and it is found that the suggested IHCP formulation has a good stability in the parameter range considered in this study. The work presented in this paper suggests a stable IHCP formulation and provides some guidelines for optimal experimental design in manufacturing and heat treatment.

Acknowledgments

The work presented in this paper was funded by the U.S. Army Program Executive Office for Simulation, Training, and Instrumentation under project no. W900KK-08-C-002, directed by Amit Kapadia and Minh Vuong. The authors would like to express their gratitude to James L. Griggs for his valuable discussions.

References

[1] dell'Erba, M., Galantucci, L. M., and Miglietta, S., "An Experimental Study on Laser Drilling and Cutting of Composite Materials for the Aerospace Industry Using Excimer and CO_2 Sources," *Composites Manufacturing*, Vol. 3, No. 1, 1992, pp. 14–19. doi:10.1016/0956-7143(92)90178-W

[2] Beck, J. V., Blackwell, B., and St. Clair, C. R., *Inverse Heat Conduction: Ill Posed Problems*, Wiley, New York, 1985.

[3] Alifanov, O. M., *Inverse Heat Transfer Problems*, Springer–Verlag, Berlin, 1994.
[4] Özisik, M. N., and Orlande, H. R. B., *Inverse Heat Transfer: Fundamentals and Applications*, Taylor and Francis, New York, 2000.
[5] Diller, T. E., "Advances in Heat Flux Measurements," *Advances in Heat Transfer*, Vol. 23, Academic Press, London, 1993, pp. 279–368.
[6] Childs, P. R. N., Greenwood, J. R., and Long, C. A., "Heat Flux Measurement Techniques," *Proceedings of the Institute of Mechanical Engineers Part C: Journal of Mechanical Engineering Science*, Vol. 213, No. 7, 1999, pp. 655–677. doi:10.1243/0954406991524471
[7] Tong, A., "Improving the Accuracy of Temperature Measurements," *Sensor Review*, Vol. 21, No. 3, 2001, pp. 193–198. doi:10.1108/02602280110398044
[8] Childs, P. R. N., "Advances in Temperature Measurement," *Advances in Heat Transfer*, Vol. 36, Elsevier Science, New York, 2002, pp. 111–181.
[9] Saidi, A., and Kim, J., "Heat Flux Sensor with Minimal Impact on Boundary Conditions," *Experimental Thermal and Fluid Science*, Vol. 28, No. 8, 2004, pp. 903–908. doi:10.1016/j.expthermflusci.2004.01.004
[10] Loulou, T., and Scott, E. P., "An Inverse Heat Conduction Problem with Heat Flux Measurements," *International Journal for Numerical Methods in Engineering*, Vol. 67, No. 11, 2006, pp. 1587–1616. doi:10.1002/nme.1674
[11] Sparrow, E. M., Haji-Sheikh, A., and Lundgren, T. S., "The Inverse Problem in Transient Heat Conduction," *Journal of Applied Mechanics*, Vol. 86, No. 3, 1964, pp. 369–375.
[12] Jarny, Y., Özisik, M. N., and Bardon, J. P., "A General Optimization Method Using Adjoint Equation for Solving Multidimensional Inverse Heat Conduction," *International Journal of Heat and Mass Transfer*, Vol. 34, No. 11, 1991, pp. 2911–2919. doi:10.1016/0017-9310(91)90251-9
[13] Pasquetti, R., and Niliot, C. L., "Boundary Element Approach for Inverse Heat Conduction Problems: Application to a Bidimensional Transient Numerical Experiment," *Numerical Heat Transfer, Part B: Fundamentals*, Vol. 20, No. 2, 1991, pp. 169–189. doi:10.1080/10407799108945000
[14] Yang, C.-Y., and Chen, C.-K., "The Boundary Estimation in Two-Dimensional Inverse Heat Conduction Problems," *Journal of Physics D: Applied Physics*, Vol. 29, No. 2, 1996, pp. 333–339. doi:10.1088/0022-3727/29/2/009
[15] Huang, C.-H., and Wang, S.-P., "A Three-Dimensional Inverse Heat Conduction Problem in Estimating Surface Heat Flux by Conjugate Gradient Method," *International Journal of Heat and Mass Transfer*, Vol. 42, No. 18, 1999, pp. 3387–3403. doi:10.1016/S0017-9310(99)00020-4
[16] Emery, A. F., Nenarokomov, A. V., and Fadale, T. D., "Uncertainties in Parameter Estimation: the Optimal Experimental Design," *International Journal of Heat and Mass Transfer*, Vol. 43, No. 18, 2000, pp. 3331–3339. doi:10.1016/S0017-9310(99)00378-6
[17] Monde, M., Arima, H., and Mitsutake, Y., "Estimation of Surface Temperature and Heat Flux Using Inverse Solution for One-Dimensional Heat Conduction," *Journal of Heat Transfer*, Vol. 125, No. 2, 2003, pp. 213–223. doi:10.1115/1.1560147
[18] Xue, X., Luck, R., and Berry, J. T., "Comparisons and Improvements Concerning the Accuracy and Robustness of Inverse Heat Conduction Algorithms," *Inverse Problems in Science and Engineering*, Vol. 13, No. 2, 2005, pp. 177–199. doi:10.1080/1068276042000303206
[19] Frankel, J. I., Osborne, G. E., and Taira, K., "Stabilization of Ill-Posed Problems through Thermal Rate Sensors," *Journal of Thermophysics and Heat Transfer*, Vol. 20, No. 2, 2006, pp. 238–246. doi:10.2514/1.9136
[20] Zhou, J., Zhang, Y., Chen, J. K., and Smith, D. E., "A Nonequilibrium Thermal Model for Rapid Heating and Pyroloysis of Organic Composites," *Journal of Heat Transfer*, Vol. 130, No. 6, 2008, p. 064501. doi:10.1115/1.2897337
[21] Matsumoto, M., and Nishimura, T., "Mersenne Twister: a 623-Dimensionally Equidistributed Uniform Pseudorandom Number Generator," *ACM Transactions on Modeling and Computer Simulation*, Vol. 8, No. 1, 1998, pp. 3–30. doi:10.1145/272991.272995